Environmental Pollution 266 (2020) 115346

Contents lists available at ScienceDirect

Environmental Pollution

journal homepage: www.elsevier.com/locate/envpol

Evaluating the meteorological normalized $PM_{2.5}$ trend (2014–2019) in the "2+26" region of China using an ensemble learning technique☆

Linglu Qu [a], Shijie Liu [a, *], Linlin Ma [a], Zhongzhi Zhang [a], Jinhong Du [a], Yunhong Zhou [b], Fan Meng [a]

[a] State Key Laboratory of Environmental Criteria and Risk Assessment, Chinese Research Academy of Environmental Sciences, Beijing, 100012, China
[b] State Key Laboratory of Environmental Geochemistry, Institute of Geochemistry, Chinese Academy of Science, Guiyang, 550081, China

ARTICLE INFO

Article history:
Received 1 May 2020
Received in revised form
18 July 2020
Accepted 29 July 2020
Available online 12 August 2020

Keywords:
$PM_{2.5}$
Meteorological confounding
Emission abatement
Boosted regression tree model

ABSTRACT

In recent years, implementation of aggressive and strict clean air policies has resulted in significant decline in observed $PM_{2.5}$ concentration in the Beijing–Tianjin–Hebei (BTH) region and its surrounding areas (i.e., the "2 + 26" region). To eliminate the effects of interannual and seasonal meteorological variation, and to evaluate the effectiveness of emission abatement policies, we applied a boosted regression tree model to remove confounding meteorological factors. Results showed that the annual average PM2.5 concentration normalized by meteorology for the "2 + 26" region declined by 38% during 2014–2019 (i.e., from 96 to 60 μg/m^3); however, the BTH region exhibited the most remarkable decrease in $PM_{2.5}$ concentration (i.e., a 60% reduction). Certain seasonal trend in normalized $PM_{2.5}$ level remained for four target subregions owing to the effects of anthropogenic emissions in autumn and winter. Although strong interannual variations of meteorological conditions were unfavorable for pollutant dispersion during the heating seasons of 2016–2018, the aggressive abatement policies were estimated to have contributed to reductions in normalized $PM_{2.5}$ concentration of 19%, 10%, 19%, and 17% in the BTH, Henan, Shandong, and Shanxi subregions, respectively. Our study eliminated the meteorological contribution to concentration variation and confirmed the effectiveness of the implemented clean air policies.

1. Introduction

Rapid industrialization and urbanization in China over the past several decades have resulted in sharply increased energy consumption, and the associated air pollution has changed dramatically (Tian et al., 2007). In recent years, severe and frequent episodes of $PM_{2.5}$ (fine particulate matter with aerodynamic diameter of <2.5 μm) pollution that threaten public health have become notable problems in China (An et al., 2019; Zhang et al., 2012). Epidemiological studies have documented that cardiovascular mortality, lung cancer, and respiratory infection are associated with long-term or short-term $PM_{2.5}$ exposure (Crouse et al., 2012; Guo et al., 2016; Maji et al., 2018; Pascal et al., 2014; Pope et al., 2011).

In January 2013, the concentration of hourly $PM_{2.5}$ was at its highest level ever recorded in Beijing (886 μg/m^3), which captured worldwide attention. Thereafter, China's State Council released the "Action Plan for the Prevention and Control of Air Pollution" for long-term air quality improvement (Chinese State Council, 2013). Although significant reductions of the annual average and peak $PM_{2.5}$ concentrations were achieved in key regions during 2013–2017 (An et al., 2019; Ding et al., 2019), $PM_{2.5}$ concentration remained at a high level during heavy pollution episodes, especially in the Beijing–Tianjin–Hebei (BTH) region (Zhang et al., 2019b). To further reduce $PM_{2.5}$ concentration during heavy pollution episodes through interregional prevention and control, the Ministry of Ecology and Environment of the People's Republic of China released the "2017 Air Pollution Prevention and Control Action Plan for the Beijing–Tianjin–Hebei region and its Surrounding Areas" (MEP, 2017). Simultaneously, a number of regulatory measures were implemented to reduce pollutant emissions, e.g., the closure of small polluting factories, replacement of coal by natural gas for winter heating, and restrictions on vehicular use through license plate rules.

☆ This paper has been recommended for acceptance by Pavlos Kassomenos.

* Corresponding author.
E-mail address: liusj@craes.org.cn (S. Liu).

https://doi.org/10.1016/j.envpol.2020.115346
0269-7491/

The issue of greatest concern for the government, policymakers, and public is the effectiveness of the policies and measures introduced. However, meteorology drives the daily, seasonal, and interannual variations in pollutant concentrations (Barmpadimos et al., 2011; Grange et al., 2018; Liang et al., 2015; Zhang et al., 2017). For example, during 2014–2019, high concentrations of $PM_{2.5}$ in Beijing were usually accompanied by low wind speeds and high humidity, especially in winter (Fig. S1). It is difficult to interpret the actual changes of pollutant concentrations within observational records, which complicates evaluation of those strategies implemented for air quality management. Therefore, it is essential to decouple the effects of meteorology on pollutant concentrations.

Chemical transport models have been used widely to assess the impact of emission control measures on pollutant concentrations (Cai et al., 2017; Cheng et al., 2019; Daskalakis et al., 2016; Tang et al., 2017; Wang et al., 2014; Zhang et al., 2019a). However, the considerable uncertainties in emission inventories and the inherent problems of chemical transport models inevitably lead to under/overestimation of pollutant concentrations that cannot be neglected (Chen et al., 2019; Geng et al., 2015). Various statistical models offer alternative ways to detrend meteorological effects (Barmpadimos et al., 2011; Grange et al., 2018; Liang et al., 2015), e.g., multiple linear regression models (Zhai et al., 2019), generalized additive models (Barmpadimos et al., 2011; Dominici et al., 2002), Bayesian hierarchical space–time models (Sahu et al., 2006), and nonparametric kernel regression (Chen et al., 2018; Liang et al., 2016; Zhang et al., 2017). Atmospheric dilution and dispersion processes are known to be complex and nonlinear. Consequently, the effects of interactions between pollutant concentrations and meteorological variables make the use of statistical models burdensome.

More recently, to separate meteorological effects from the observed changes in pollutant concentrations, methods adopting decision trees have been developed, e.g., boosted regression tree (BRT) models (Carslaw and Taylor, 2009) and random forest models (Grange et al., 2018). A BRT model outperforms most traditional statistical models in terms of predictive performance because it incorporates the fitting and combining of many simpler models for prediction purposes (Elith et al., 2008). The predictive power of a BRT makes it suitable for modeling short-term pollutant concentrations. A BRT incorporates simultaneously two important advantages of tree-based methods: the ability to handle different types of variable and the capacity to accommodate missing data (De'ath, 2007; Elith et al., 2008). Moreover, there is no need for prior transformation of the data or the removal of outliers for model fitting. A BRT can be used to model complex nonlinear relationships between variables, and it allows the effects of interaction between variables to be quantified and visualized (Carslaw et al., 2012).

In this study, we applied a BRT model to conduct meteorological normalization of $PM_{2.5}$ concentrations in the BTH region and its surrounding areas (i.e., the "2 + 26" region). This study 1) evaluated the changes of observed and normalized $PM_{2.5}$ concentrations from 2014 to 2019, 2) presented the temporal variations of observed and normalized $PM_{2.5}$ concentrations in four target subregions, and 3) quantified the roles of meteorological conditions and anthropogenic emissions on $PM_{2.5}$ concentrations in the heating seasons.

2. Meteorological normalization methods and monitoring data

2.1. Study sites

The "2 + 26" region comprises two municipalities (i.e., Beijing and Tianjin) and 26 other adjacent cities surrounding Beijing. As shown in Fig. 1, the 28 cities comprise Shijiazhuang, Baoding, Langfang, Tangshan, Cangzhou, Hengshui, Handan, and Xingtai in Hebei Province; Taiyuan, Yangquan, Changzhi, and Jincheng in Shanxi Province; Jinan, Zibo, Liaocheng, Dezhou, Binzhou, Jining, and Heze in Shandong Province; and Zhengzhou, Xinxiang, Hebi, Anyang, Jiaozuo, Puyang, and Kaifeng in Henan Province. Most are industrial cities that consume large volumes of coal and produce enormous quantities of airborne pollutants. Additionally, the unfavorable geography that is characterized by the Yanshan Mountains to the north and the Taihang Mountains to the west is ideal for secondary generation of $PM_{2.5}$ in the "2 + 26" region. The combination of the large volume of emissions and the special weather conditions make this region one of the areas of China with the poorest air quality.

2.2. Data

Daily data of surface air $PM_{2.5}$ concentration during 2014–2019 in the 28 cities were collected from the China National Environmental Monitoring Center. The daily average concentration of each city was calculated by averaging the hourly value measured at all

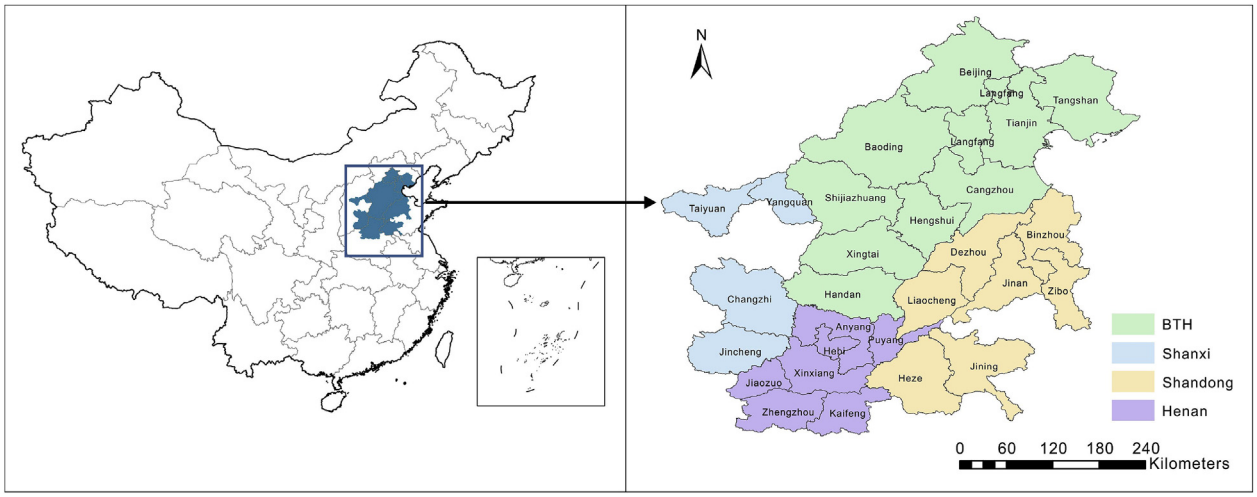

Fig. 1. Location of the study area and the classification of four geographical regions in the "2 + 26" region.

available "Guokong" monitoring sites within the city. Data from "Guokong" monitoring sites are managed directly by the Ministry of Ecology and Environment of the People's Republic of China to avoid local interference.

We correlated the $PM_{2.5}$ data with meteorological data of the corresponding period to investigate meteorological confounding. Meteorological data, collected from the National Meteorological Information Center, included temperature (T, °C), relative humidity (RHU, %), precipitation (P, mm), sunshine duration (SSD, h), air pressure (PRE, Pa), surface temperature (GST, °C), wind speed (WS, m/s), and wind direction (WD). The wind direction was divided into 16 directions: N, NNE, NE, ENE, E, ESE, SE, SSE, S, SSW, SW, WSW, W, WNW, NW, and NNW. Data were analyzed in R using the deweather package (Carslaw and Taylor, 2009).

In this study, we compiled a $PM_{2.5}$ and meteorological data set covering 61,348 d. There were 1094 missing $PM_{2.5}$ data, primarily during 2014 in Hebi, Puyang, and Xinxiang. Therefore, we only considered the period 2015–2018 when analyzing air pollution in the heating seasons. The heating season in China refers to the period from October of one year to March of the following year.

2.3. Modeling and meteorological normalization

The flow diagram presented in Fig. 2 shows that the data modeling and analysis comprised two steps: the BRT model was built first and then meteorological normalization was conducted. The modeling process requires three main parameters, e.g., learning rate, number of trees, and interaction depth. In this study, the learning rate of 0.1, number of trees of 1000, and interaction depth of 6 were used.

All observed data were divided randomly into two groups: a training set that accounted for 80% of all data and a testing set that comprised the remaining 20% of the data. The training set and input independent variables were used to grow a sequence of trees. The independent variables included temporal variables (weekday, week, month, and trend term) and meteorological parameters (WS, WD, T, RHU, P, SSD, PRE, and GST). The basic idea of a BRT is to fit iteratively a collection of weak learners to form a strong learner (De'ath, 2007). In boosting, the model grows a sequence of trees starting from a constant prediction. In each following step, a new tree is added progressively. For example, a new tree is fitted to the residual of the first tree in the second step. Then, the reweighted data are used to fit the next tree, and so on (Elith et al., 2008). This forward stagewise process means only those fitted values predicted poorly by the previous trees are reestimated, while existing trees remain unchanged. This process can be represented as follows:

$$y_i = \sum_{k=1}^{K} f_k(x_i),\ f_k \in F \tag{1}$$

$$y_i^{(0)} = 0$$

$$y_i^{(1)} = f_1(x_i) = y_i^{(0)} + f_1(x_i)$$

$$y_i^{(2)} = f_1(x_i) + f_2(x_i) = y_i^{(1)} + f_2(x_i)\ldots$$

$$y_i^{(t)} = \sum_{k=1}^{t} f_k(x_i) = y_i^{(t-1)} + f_t(x_i) \tag{2}$$

where y_i is the sum of models with k trees, $y_i^{(t)}$ is the model at boosting round t, $y_i^{(t-1)}$ is the reserved tree added in the previous

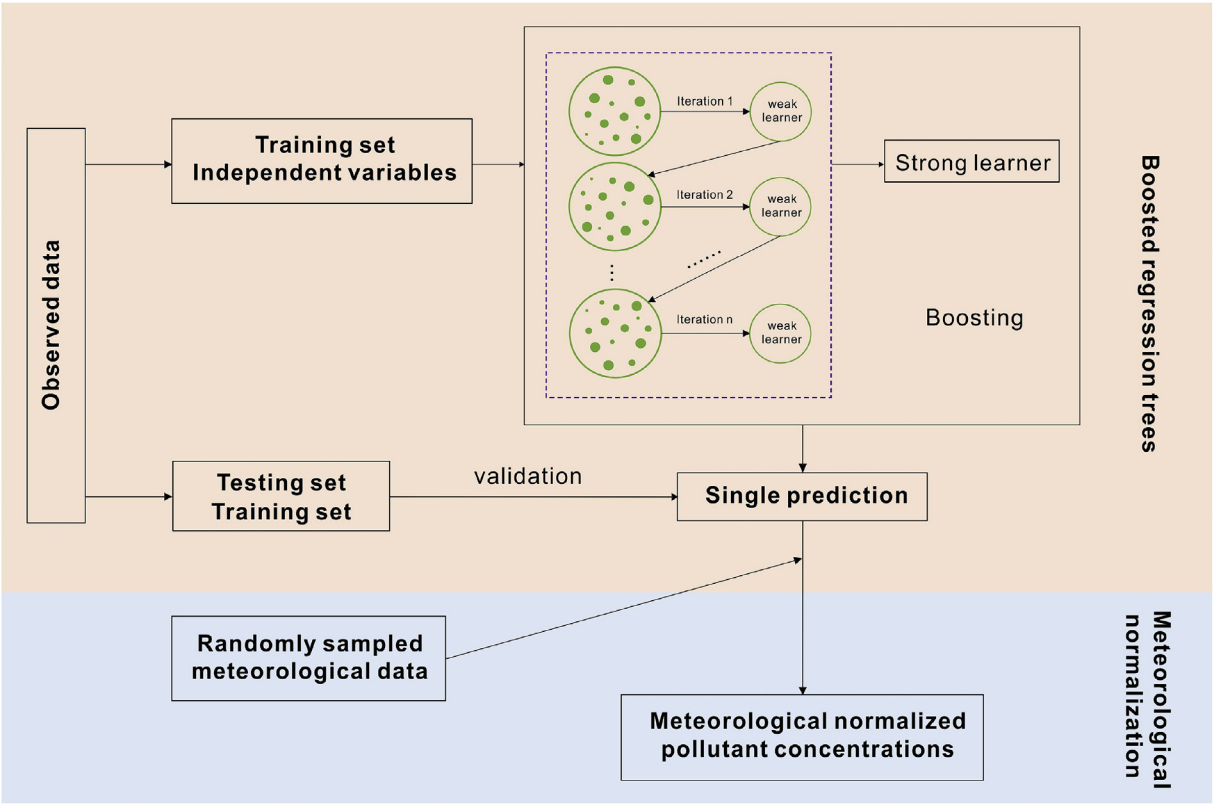

Fig. 2. A diagram of analysis model.

round, and $f_t(x_i)$ is a new tree.

In this study, the iterative process was repeated 1000 times. The predictions were aggregated by averaging to produce an overall prediction. In this work, the training and testing sets were used to validate the performance of the BRT model through a cross-validation procedure. Model evaluation was based on common statistical indices that included the root mean square error (RMSE), Pearson correlation coefficient (R), fraction of predictions within a factor of two (FAC2), mean bias (MB), mean gross error (MGE), normalized mean bias (NMB), normalized mean gross error (NMGE), coefficient of efficiency (COE), and index of agreement (IOA) (Carslaw, 2015). The formulas of these indices, in which O_i and P_i represent the i-th observed and predicted values for a total of n observations, respectively, are given as follows:

$$RMSE = \sqrt{\left(\frac{\sum_{i=1}^{n}(P_i - O_i)^2}{n}\right)} \tag{3}$$

$$R = \frac{1}{(n-1)}\sum_{i=1}^{n}\left(\frac{P_i - \overline{P}}{\sigma_P}\right)\left(\frac{O_i - \overline{O}}{\sigma_O}\right) \tag{4}$$

$$FAC2 = 0.5 \le \frac{P_i}{O_i} \le 2.0 \tag{5}$$

$$MB = \frac{1}{n}\sum_{i=1}^{n}(P_i - O_i) \tag{6}$$

$$MGE = \frac{1}{n}\sum_{i=1}^{n}|P_i - O_i| \tag{7}$$

$$NMB = \frac{\sum_{i=1}^{n}P_i - O_i}{\sum_{i=1}^{n}O_i} \tag{8}$$

$$NMGE = \frac{\sum_{i=1}^{n}|P_i - O_i|}{\sum_{i=1}^{n}O_i} \tag{9}$$

$$COE = 1.0 - \frac{\sum_{i=1}^{n}|P_i - O_i|}{\sum_{i=1}^{n}|O_i - \overline{O}|} \tag{10}$$

$$IOA = \begin{cases} 1.0 - \dfrac{\sum_{i=1}^{n}|P_i - O_i|}{c\sum_{i=1}^{n}|O_i - \overline{O}|}, \ when \\ \sum_{i=1}^{n}|P_i - O_i| \le c\sum_{i=1}^{n}|O_i - \overline{O}| \\ \qquad\qquad\qquad\qquad , \ with\ c = 2 \\ \dfrac{c\sum_{i=1}^{n}|O_i - \overline{O}|}{\sum_{i=1}^{n}|P_i - O_i|} - 1.0, \ when \\ \sum_{i=1}^{n}|P_i - O_i| > c\sum_{i=1}^{n}|O_i - \overline{O}| \end{cases} \tag{11}$$

The RMSE provides a reasonable overall measure of the deviation between observed and predicted values. R is the measure of the linear relationship between two variables; the closer the value of R is to +1 or −1, the stronger the correlation between the two variables. An R value of zero means the two variables have no correlation. FAC2 is a robust performance measure because it is unaffected by outliers. The fraction of the model prediction needs to satisfy the condition in Eq. (5). A model is considered to satisfy the condition when the FAC2 value approaches 1 (Suleiman et al., 2016). MB and MGE are two common measures used to quantify the deviation between predicted and observed values. An MB of zero indicates an ideal model. NMB and NMGE are the normalized versions of MB and MGE, respectively. They also represent the mean paired prediction−observation differences. Unlike MB and MGE, NMB and NMGE can compare pollutants that cover different ranges of concentration. Both are unbounded at the positive (upper) end but bounded at −100% for NMB and 0% for NMGE at the lower end (Yu et al., 2006). For both indices, a value of zero indicates no over-/underestimation by the model. COE is a measure of the prediction accuracy of a model. A perfect model has a COE value of 1; zero and negative COE values indicate that the prediction accuracy of the model is no greater than and worse than the observed mean, respectively (Legates and McCabe, 2013). The IOA is a relative and bounded measure proposed by Willmott (1982) that is applied widely in model evaluation. IOA values range from −1 to +1 with values toward the latter indicating better model performance.

The meteorological normalization of daily $PM_{2.5}$ concentration in a specific city was derived by repeated prediction with a random sampling of meteorological parameters. Specifically, the temporal variables and meteorological parameters were selected at random to form a new data set that was then used as input for the BRT model to predict $PM_{2.5}$ concentration. The process was repeated 1000 times. Finally, all predicted values were aggregated to calculate an average, i.e., the so-called meteorological normalized $PM_{2.5}$ concentration. The normalized concentrations for each city were considered comparable over the studied years because they were calculated under a comparable baseline meteorological equilibrium of the city.

2.4. Contributions of meteorological conditions and anthropogenic emissions to $PM_{2.5}$ concentration variation

The interannual rates of change of $PM_{2.5}$ concentrations, based on their original concentrations, are affected by three factors, i.e., the meteorological conditions of a target year and the previous year and the variation of anthropogenic emissions. Therefore, we combined observed and normalized concentrations for accurate quantification and evaluation of the meteorological and emission abatement effects (Environmental statistics group in Center for Statistical Science (2019)):

$$\frac{x_2 - x_1}{x_1} = \frac{x_2 - \widetilde{x_2}}{x_1} + \frac{\widetilde{x_2} - \widetilde{x_1}}{x_1} + \frac{\widetilde{x_1} - x_1}{x_1} \tag{12}$$

where x_1 and $\widetilde{x_1}$ represent the observed and normalized $PM_{2.5}$ concentrations of the previous year, respectively, and x_2 and $\widetilde{x_2}$ represent the observed and normalized $PM_{2.5}$ concentrations of the target year, respectively. Therefore, $\frac{x_2 - \widetilde{x_2}}{x_1}$ and $\frac{\widetilde{x_1} - x_1}{x_1}$ reflect the meteorological effects of the target year and the previous year, respectively, on the rate of change of observed $PM_{2.5}$ concentrations, where positive and negative values represent unfavorable and favorable meteorological conditions, respectively. Moreover, $\frac{\widetilde{x_2} - \widetilde{x_1}}{x_1}$ reflects the effect of anthropogenic emissions of the target on the rate of change of observed $PM_{2.5}$ concentrations, where positive and negative values represent increased and decreased anthropogenic emissions in the target year, respectively.

Table 1
Test results of model performance.

	Test set	Training set
RMSE	30.97	28.14
R	0.83**	0.86**
FAC2	0.92	0.93
MB	0.08	0.00
MGE	20.67	19.41
NMB	0.00	0.00
NMGE	0.28	0.27
COE	0.77	0.80
IOA	0.83	0.85

Note: $^{**}P < 0.01$ indicates that predicted values are significantly correlated with observed values.

3. Results and discussion

3.1. Evaluation of model performance

Nine statistical indices were used to evaluate our model in different ways. The statistical results of model performance are shown in Table 1. The high R values for the test set (0.83) and the training set (0.86) indicate that the relation between the predicted values and the observed values was significant. This conclusion is also supported by the test r^2 value of 0.69 and the training r^2 of value 0.75 shown in Fig. 3. FAC2 values of 0.92 and 0.93 were found for the test set and the training set, respectively, which suggest that our model satisfies the condition for the fraction of predictions. MB values of 0.08 and 0 show that the bias produced by our model was very small. Similarly, the lower values of NMB and NMGE indicate that our model performed well. The differences in the COE and IOA values for the test set and the training set were very small. It was considered that our model had satisfactory prediction capability, as verified by all the indices.

3.2. Observed $PM_{2.5}$ trends in the "2 + 26" region during 2014–2019

$PM_{2.5}$, which is a major urban air pollutant, replaced PM_{10} as the primary air pollutant in China in 2013 (Liang et al., 2016). In previous years, North China has experienced severe and persistent haze pollution episodes with large spatiotemporal coverage, particularly on the North China Plain, and various environmental regulations have been promoted from the central to local governments to improve air quality (An et al., 2019). Following such measures, significant decreases were observed in $PM_{2.5}$ concentrations during 2014–2019 (except 2017) in the "2 + 26" region (Fig. 4A). The annual average $PM_{2.5}$ concentration in 2014–2019 was 94, 83, 76, 70, 60, and 57 μg/m^3, respectively. Compared with 2014, the regional annual average $PM_{2.5}$ concentration in 2019 represented a decline of 39%. In 2018, the highest decline in annual average $PM_{2.5}$ concentration was observed with a 14% year-on-year decrease.

It can be seen in Fig. 1 that the 28 cities in the "2 + 26" region could be grouped into four target subregions, i.e., the BTH, Henan, Shandong, and Shanxi subregions. To eliminate the interference of $PM_{2.5}$ concentration fluctuations and more accurately analyze their seasonal differences, $PM_{2.5}$ concentrations in the four target subregions were standardized. The Standardization is defined as $PM_{2.5}$ concentration minus the mean $PM_{2.5}$ concentration, and then divided by the standard deviation (i.e., ($PM_{2.5}$-mean)/sd). The seasonal trend of observed $PM_{2.5}$ level for each subregion is shown in Fig. 5A. There was significant seasonal trend in $PM_{2.5}$ level in all subregions, with higher levels in autumn and winter and lower levels in spring and summer. Previous research has demonstrated that this seasonality is attributable partly to unfavorable meteorological conditions (Chen et al., 2019; Zhai et al., 2019; Zhang et al., 2019b) and partly to heating effects (Liu et al., 2016; Xiao et al., 2015).

3.3. Normalized $PM_{2.5}$ trends in the "2 + 26" region during 2014–2019

Recent studies have reported the impact of meteorological conditions on observed pollutant concentrations (Carslaw et al., 2012; Grange et al., 2018; Liang et al., 2016; Zhang et al., 2019a). It is necessary to account for meteorological confounding factors when evaluating air quality improvements and the effectiveness of emission reduction policies (Carslaw and Taylor, 2009; Henneman et al., 2017). We applied the approach proposed in Carslaw and Taylor (2009) to remove the meteorological effects and to

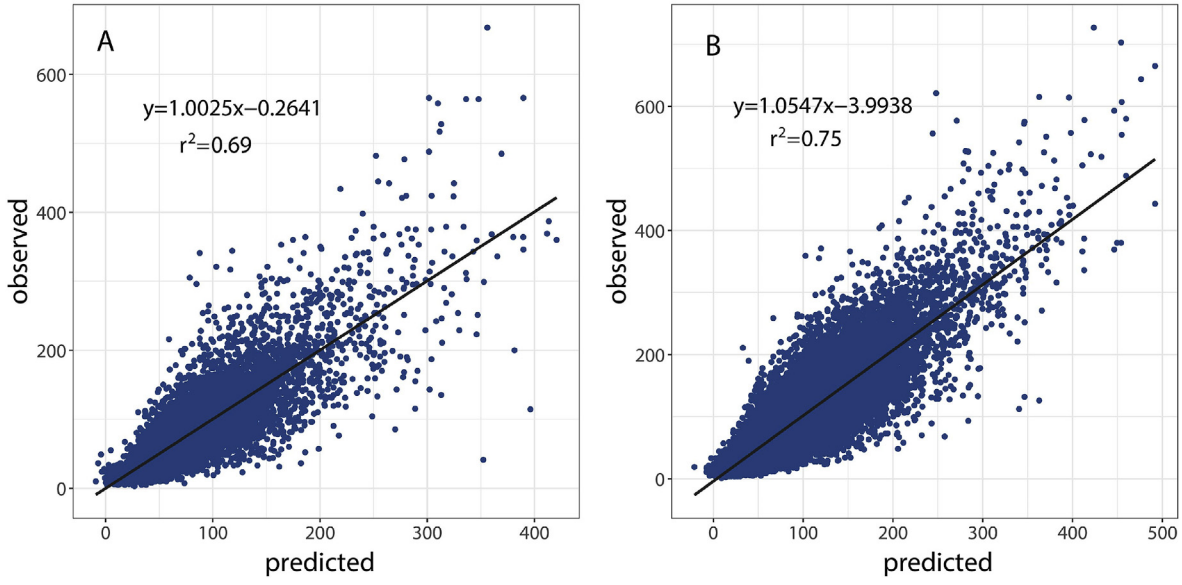

Fig. 3. Evaluation of the performance of the boosted regression tree model by using cross-validation. (A) test set and (B) training set.

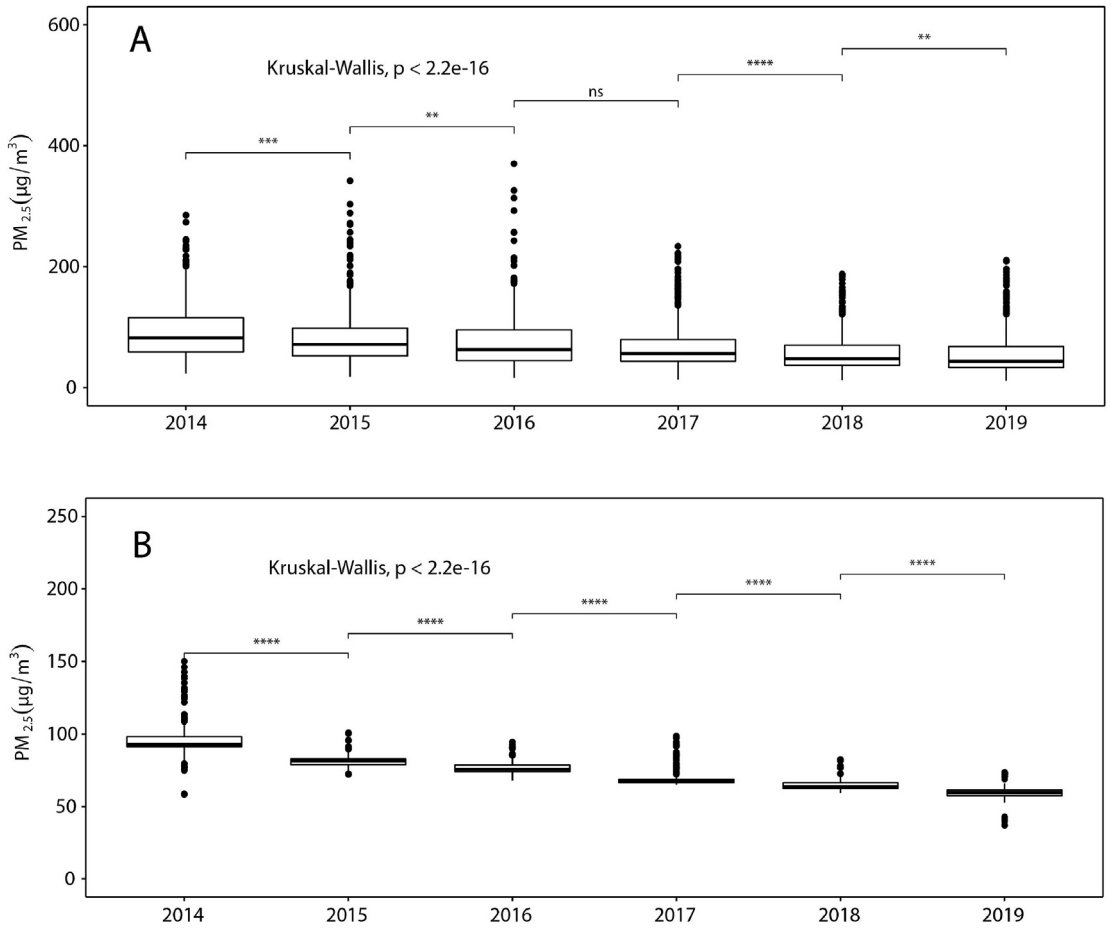

Fig. 4. The interannual variations of $PM_{2.5}$ concentration in "2 + 26" region from 2014 to 2019. (A) Observed annual average $PM_{2.5}$ concentration. (B) Normalized annual average $PM_{2.5}$ concentration. (**** indicates that the change of $PM_{2.5}$ concentration is highly significant, *** and ** indicate that the change of $PM_{2.5}$ concentration is significant, and ns indicates that there is no significant change in $PM_{2.5}$ concentration.)

calculate the meteorological normalized $PM_{2.5}$ concentrations. As shown in Fig. 4B, the normalized $PM_{2.5}$ concentration decreased significantly every year across the entire region. The annual average normalized $PM_{2.5}$ concentration during 2014–2019 was 96, 81, 77, 70, 65, and 60 μg/m^3, respectively. The highest concentration also showed a steady decrease from 108 μg/m^3 in 2014 to 66 μg/m^3 in 2019. The interannual decline in the rate of highest $PM_{2.5}$ concentration during 2014–2019 was 18%, 4%, 15%, 0%, and 8%, respectively.

After removal of meteorological effects, the $PM_{2.5}$ level in the four target subregions still varied seasonally (Fig. 5B). Compared with the observed $PM_{2.5}$ level, the normalized $PM_{2.5}$ level decreased significantly during 2014–2019. However, the normalized $PM_{2.5}$ level rebounded obviously in the BTH subregion in the autumn and winter of 2016 in comparison with that in the autumn and winter of 2015.This was largely consistent with a rebound in the consumption of coal by the metal, steel, iron, and electricity sectors in Hebei during the same period (Chen et al., 2018). As shown in Table 2, the normalized annual average $PM_{2.5}$ concentration in the BTH, Shandong, and Henan subregions declined steadily. Relative trends in the BTH, Shandong, and Henan subregions were −10%/a, −10%/a, and −6%/a, respectively, during 2014–2019. However, the trend in Shanxi rebounded in 2015–2016 and plateaued in 2016–2017. The more remarkable decrease in normalized $PM_{2.5}$ level over a longer time span was found in the BTH subregion. For example, it dropped from 139 μg/m^3 in January 2014 to 56 μg/m^3 in December 2019, representing a 60% reduction. In this subregion, the normalized $PM_{2.5}$ concentration in Beijing also improved year by year. The annual average normalized $PM_{2.5}$ concentration during 2014–2019 was 81, 73, 70, 60, 54, and 48 μg/m^3, respectively. These values are similar to those of Vu et al. (2019), who reported that the normalized $PM_{2.5}$ concentration in Beijing during 2014–2017 was 85, 75, 71, and 61 μg/m^3, respectively. Despite the recent dramatic decreases in normalized $PM_{2.5}$ concentration in the four target subregions, $PM_{2.5}$ concentrations remain at a level higher than the international standards, i.e., 35 μg/m^3 set by the US Environmental Protection Agency or 20 μg/m^3 set by the European Union (Chen et al., 2018).

3.4. Meteorological and anthropogenic effects on $PM_{2.5}$ in the heating seasons

We analyzed $PM_{2.5}$ levels in the heating seasons in the "2 + 26" region. As shown in Fig. 6, the observed annual $PM_{2.5}$ concentration in the BTH, Henan, Shandong, and Shanxi subregions declined by 20%, 10%, 31%, and 9% during 2015–2018, respectively. The normalized annual $PM_{2.5}$ concentration in the BTH subregion was 66 μg/m^3 in 2018, which represents a decline of 13% in comparison with the 2015 concentration. The normalized annual $PM_{2.5}$ concentration in the Henan subregion was 67 μg/m^3 in 2018, which represents a decline of 20% in comparison with the 2015 concentration. The normalized annual $PM_{2.5}$ concentration in the

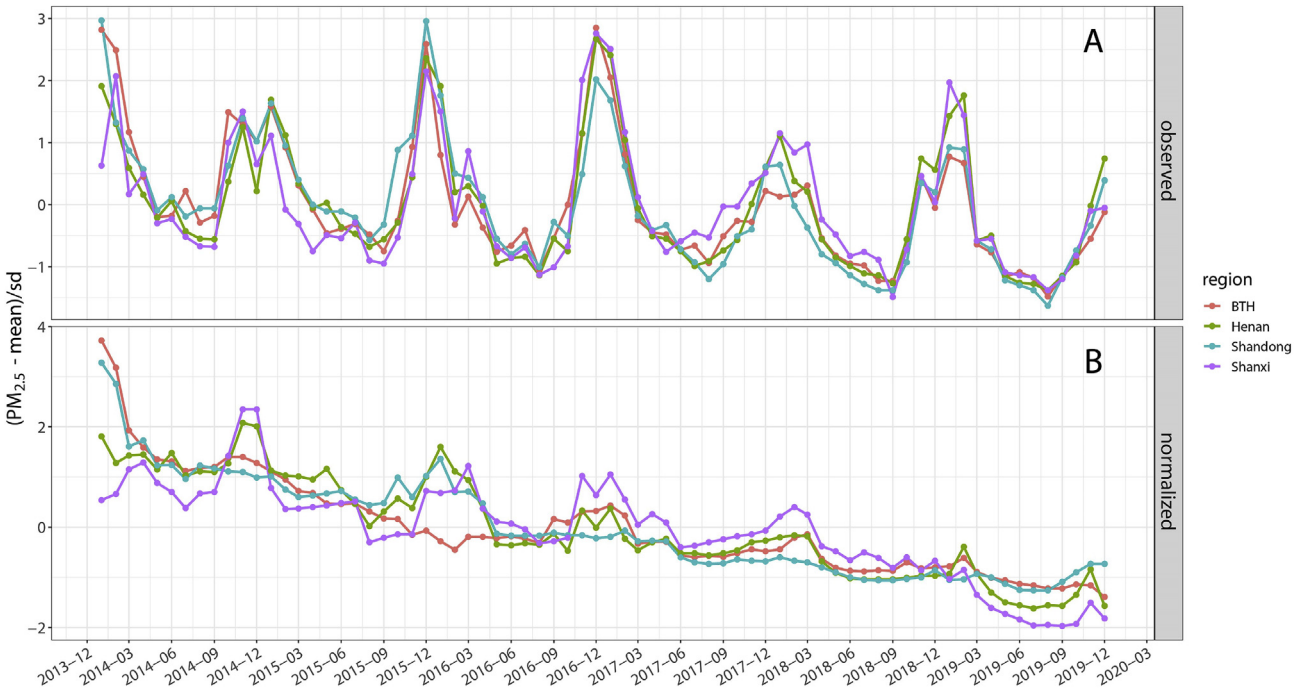

Fig. 5. Seasonal trend of $PM_{2.5}$ during 2014–2019 in the four target subregions. (A) Observed $PM_{2.5}$ level. (B) Normalized $PM_{2.5}$ level.

Table 2
Relative trends of annual average normalized $PM_{2.5}$ concentrations in the four target subregions from 2014 to 2019 (%).

	2015–2014	2016–2015	2017–2016	2018–2017	2019–2018
BTH	−19.5	−10.2	−5.0	−7.4	−9.5
Shanxi	−13.6	7.5	0.1	−5.0	−20.1
Shandong	−13.8	−10.5	−14.0	−10.2	−3.8
Henan	−7.4	−6.1	−6.3	−5.7	−6.7

Shandong subregion was 59 $\mu g/m^3$ in 2018, which represents a decline of 35% in comparison with the 2015 concentration. The normalized annual $PM_{2.5}$ concentration in the Shanxi subregion was 55 $\mu g/m^3$ in 2018, which represents a decline of 16% in comparison with the 2015 concentration. It is evident that the difference between the decrease of observed and normalized annual concentrations was much larger in the Henan subregion than in the other subregions. These differences and trends of normalized $PM_{2.5}$ reflect the effects of meteorological conditions and emission control actions.

We separated the contribution from meteorological effects from that of anthropogenic emissions. The interannual changes of meteorological conditions were notable in the heating seasons of 2016–2018 (Fig. 7A, C, and E). In the "2 + 26" region, the worst meteorological conditions occurred in 2016, followed by sharp improvement in 2017 and subsequent deterioration in 2018. However, the meteorological conditions in Beijing were favorable for $PM_{2.5}$ dispersion in both 2017 and 2018. We estimated that variation in meteorological conditions during 2016–2018 contributed to observed reductions in $PM_{2.5}$ of 20, 11, 3, and 9 $\mu g/m^3$ in the BTH, Henan, Shandong, and Shanxi subregions, respectively (Fig. 6).

Similarly, interannual changes existed in the contribution of anthropogenic emissions to ambient $PM_{2.5}$ concentrations in the heating seasons. As shown in Fig. 7B, anthropogenic emissions increased notably in the BTH subregion. Data from the National Bureau of Statistics reported year-on-year increases of 323.63×10^6 and 156.10×10^6 t in the production of pig iron and crude steel, respectively, in the 2016 heating season in the BTH subregion (Fig. S2). The anthropogenic emissions contributed to an increase of 5 $\mu g/m^3$ in the normalized $PM_{2.5}$ concentration during 2015–2016 (Fig. 6A). In 2017, aggressive and strict control actions were implemented in the "2 + 26" region, including the "Coal to Gas" project, phasing out of small and polluting factories, implementation of the ultralow emission standards for power plants, and staggered production for industries in the heating season (MEP, 2017). In the same year, the total coal consumption in the BTH subregion hit its lowest level in over a decade (Environmental statistics group in Center for Statistical Science (2019)). In comparison with the 2016 heating season, the BTH subregion experienced a dramatic decrease in anthropogenic emissions in the same period in 2017 (Fig. 7D). A reduction of 11% in the normalized $PM_{2.5}$ concentration in the BTH subregion during 2016–2017 was the result of the successful implementation of these control actions (Fig. 6A). It is evident that the decreases in anthropogenic emissions in the Henan and Shandong subregions (Fig. 7B and D) led to year-on-year decreases in normalized $PM_{2.5}$ concentration in the heating seasons of 2015–2017 (Fig. 6B and C). Their trends can be explained by the changes in the outputs of industrial products during the same period. As shown in Fig. S2, the outputs of cement, crude steel, and pig iron during 2015–2017 in the Henan subregion declined by 19%, 3%, and 16%, respectively. In the Shandong subregion, the outputs of cement and pig iron during 2015–2017 declined by 13% and 10%, respectively. However, the normalized $PM_{2.5}$ concentration in the Shanxi subregion showed an opposite trend (Fig. 6D), i.e., anthropogenic emissions increased in some cities within the Shanxi subregion in the heating seasons of 2016 and 2017 (Fig. 7B and D). In the corresponding period, steady increases in the outputs of crude steel and pig iron were evident (Fig. S2). To accelerate the improvement of air quality, further emission abatement measures, e.g., bulk coal management, the control of total coal consumption and improved energy efficiency, were required and implemented in 2018 (Chinese State Council,

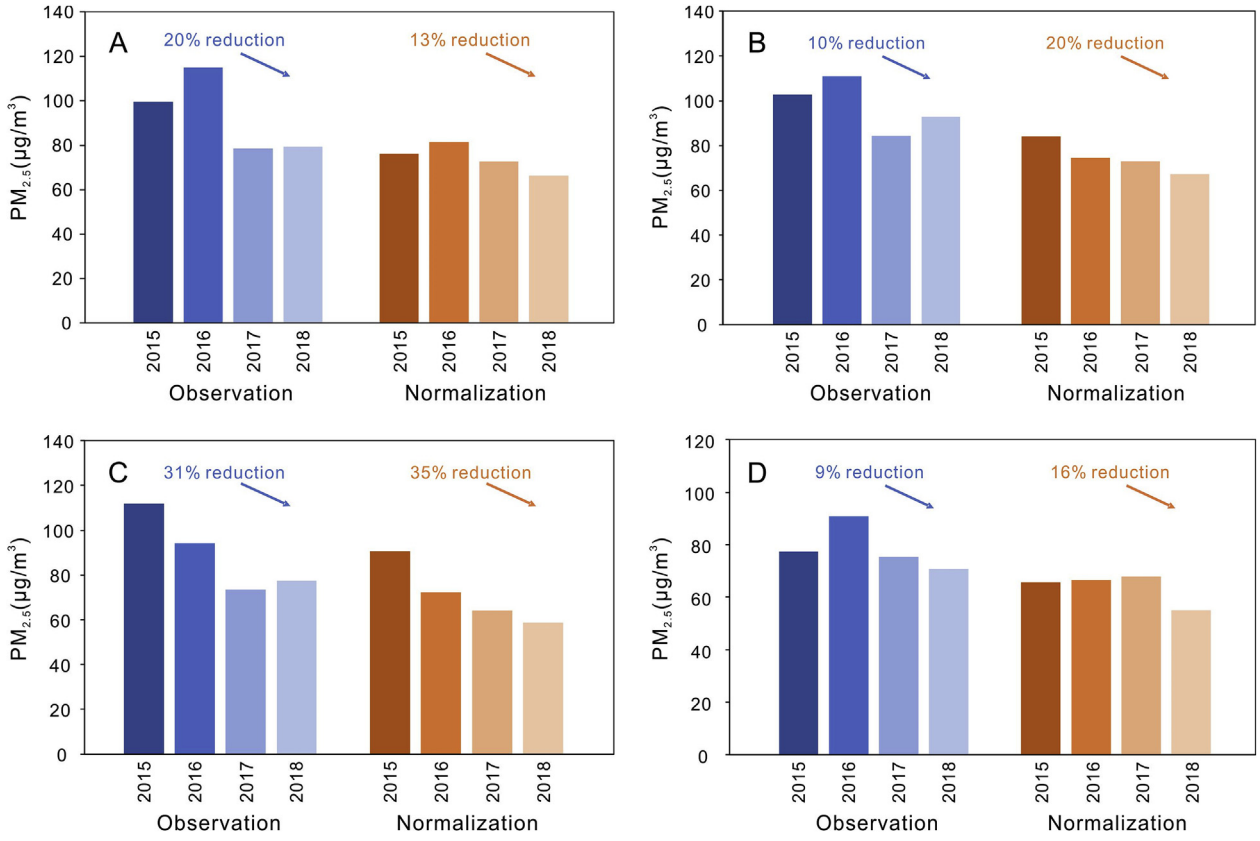

Fig. 6. Observed and normalized annual average $PM_{2.5}$ concentrations in the heating seasons from 2015 to 2018 in the four target subregions. (A)BTH, (B)Henan, (C)Shandong and (D)Shanxi.

2018). In the previous three years, the "Coal to Gas" project has led to a substantial decrease in bulk coal consumption from approximately 56 $\times$ 10^6 t/a to approximately 23 $\times$ 10^6 t/a in the "2 + 26" region (MEP, 2020). As shown in Fig. 7F, anthropogenic emissions generally continued to decline in the 2018 heating season. Accordingly, the normalized $PM_{2.5}$ concentrations in the four target subregions decreased owing to the continued abatement measures (Fig. 6), despite the rebound in the outputs of cement, crude steel, and pig iron in the 2018 heating season in the BTH, Shandong, and Shanxi subregions (Fig. S2). For three years, emission control actions led to reduced normalized $PM_{2.5}$ concentration by 15 μg/m^3 in the BTH subregion, contributing 19% of the total decrease in the normalized $PM_{2.5}$ concentration. In the same period, emission control actions led to reduced normalized $PM_{2.5}$ concentration by 7, 13, and 11 μg/m^3 in the Henan, Shandong, and Shanxi subregions, contributing 10%, 19%, and 17% of the total decrease in the normalized $PM_{2.5}$ concentration, respectively. These results indicate that aggressive abatement actions have played a role in reducing $PM_{2.5}$ levels without meteorological confounding.

4. Conclusions

During 2014–2019, air quality in the "2 + 26" region of China has improved considerably. In this period, observed $PM_{2.5}$ concentration has shown a dramatic decrease from 94 to 57 μg/m^3, driven by emission abatement policies intertwined with complex meteorological confounding. Strong meteorological effects cause confounding problems in air quality assessment. Thus, for meaningful comparison of interannual variations of $PM_{2.5}$ concentration, it is necessary to decouple the meteorological effects. This study applied a BRT model to separate and quantify the contributions of meteorological conditions and anthropogenic emissions to the variation of $PM_{2.5}$ concentrations. Nine statistical indices verified the satisfactory performance of the model.

After removal of the meteorological effects, it was found that the normalized $PM_{2.5}$ concentrations decreased significantly year-on-year in the "2 + 26" region. Overall, the annual average normalized $PM_{2.5}$ concentration declined by 38% from 96 μg/m^3 in 2014 to 60 μg/m^3 in 2019. The research area was divided into four target subregions. Compared with observed $PM_{2.5}$ levels, weak seasonal variation still appeared in the normalized $PM_{2.5}$ levels of these subregions with higher levels in autumn and winter and lower levels in spring and summer. The BTH subregion exhibited the most remarkable decrease in $PM_{2.5}$ concentration with a 60% reduction from January 2014 to December 2019. Our results confirmed that anthropogenic emissions decreased steadily in the heating seasons of 2016–2018, even if the meteorological conditions were unfavorable for pollutant dispersion. The aggressive emission control measures contributed to a reduction of 19%, 10%, 19%, and 17% in the normalized $PM_{2.5}$ concentration in the BTH, Henan, Shandong, and Shanxi subregions, respectively, in the heating seasons of 2016–2018.

The modeling work conducted in this study confirmed both the effectiveness of the clean air actions introduced by the government and the impact of strong interannual and seasonal variation of meteorological conditions. However, several challenges remain to be addressed. First, comprehensive evaluation of urban air quality will require meteorological normalization for other pollutants. Second, consideration should be given to the effect of changes in emissions of precursor pollutants for further simulation analysis of

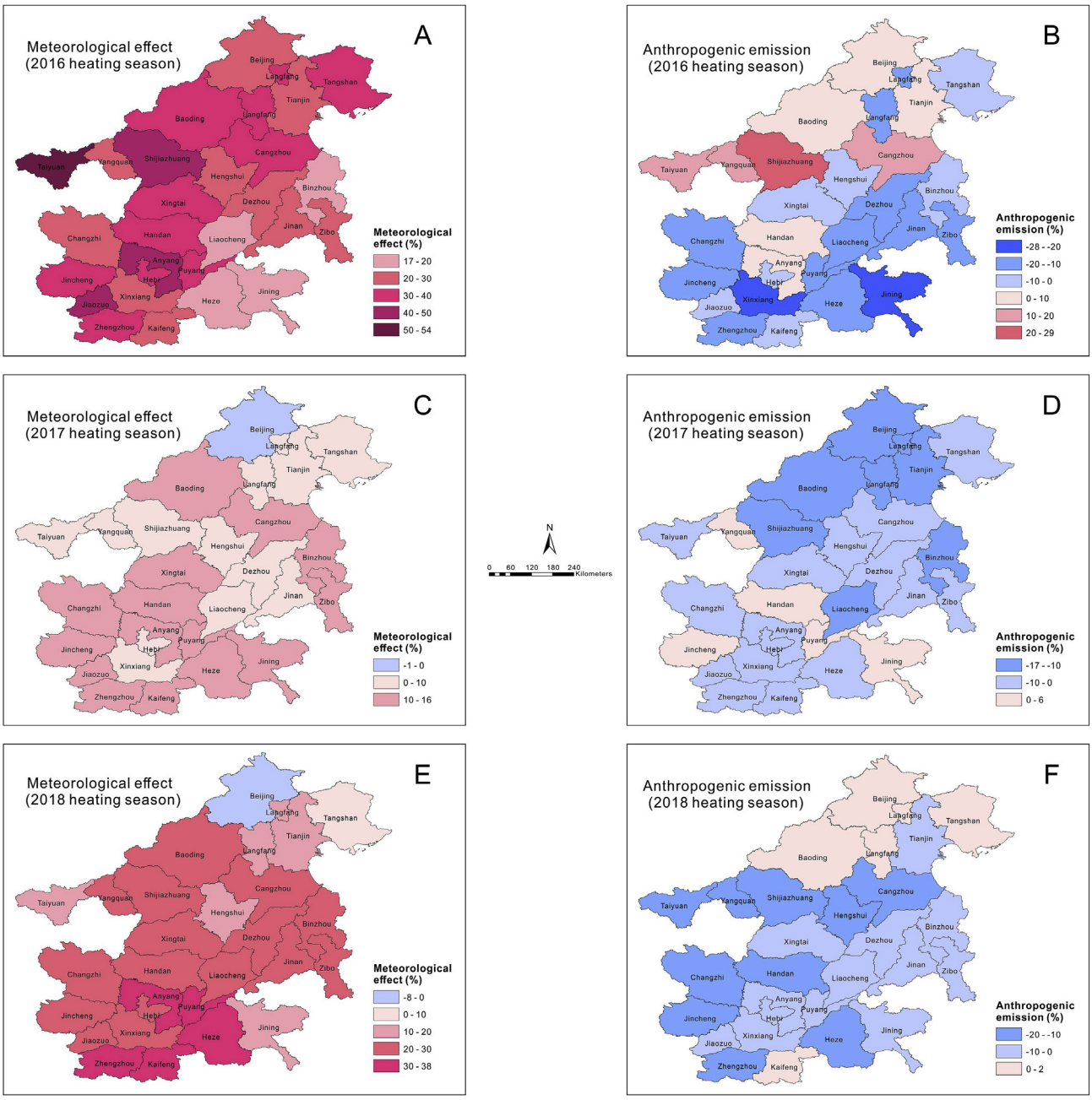

Fig. 7. Relative contributions of changes of meteorological conditions and anthropogenic emissions to $PM_{2.5}$ concentration in the heating seasons from 2016 to 2018.

ozone owing to its complex generation mechanism. Third, the contributions of specific mitigation measures to air quality improvement should be quantified. Such work would provide a sound basis for the development of regional abatement policies.

CRediT authorship contribution statement

Linglu Qu: Writing - original draft, Conceptualization, Methodology, Formal analysis, Visualization. **Shijie Liu:** Conceptualization, Writing - review & editing, Funding acquisition. **Linlin Ma:** Software, Data curation, Visualization. **Zhongzhi Zhang:** Software, Data curation. **Jinhong Du:** Investigation. **Yunhong Zhou:** Investigation. **Fan Meng:** Supervision, Writing - review & editing.

Declaration of competing interest

The authors declare that they have no known competing financial interests or personal relationships that could have appeared to influence the work reported in this paper.

Acknowledgments

This work was supported by the Natural Science Foundation of China (grant number 41701588), the National Research Program for Key Issues in Air Pollution Control (DQGG0107) and the National Key R&D Program of China (2017YFC0212100).

Appendix A. Supplementary data

Supplementary data to this article can be found online at https://doi.org/10.1016/j.envpol.2020.115346.

References

An, Z.S., Huang, R.J., Zhang, R.Y., Tie, X.X., Li, G.H., Cao, J.J., Zhou, W.J., Shi, Z.G., Han, Y.M., Gu, Z.L., Ji, Y.M., 2019. Severe haze in northern China: a synergy of anthropogenic emissions and atmospheric processes. Proc. Natl. Acad. Sci. 116, 8657–8666.

Barmpadimos, I., Hueglin, C., Keller, J., Henne, S., Prévôt, A., 2011. Influence of meteorology on PM_{10} trends and variability in Switzerland from 1991 to 2008. Atmos. Chem. Phys. 11, 1813–1835.

Cai, S.Y., Wang, Y.J., Zhao, B., Wang, S.X., Chang, X., Hao, J.M., 2017. The impact of the "air pollution prevention and control action plan" on $PM_{2.5}$ concentrations in Jing-Jin-Ji region during 2012-2020. Sci. Total Environ. 580, 197–209.

Carslaw, D.C., 2015. The Openair Manual – Open-Source Tools for Analysing Air Pollution Data. Manual for Version 1, vols. 1–4. King's College, London, pp. 231–233.

Carslaw, D.C., Taylor, P.J., 2009. Analysis of air pollution data at a mixed source location using boosted regression trees. Atmos. Environ. 43, 3563–3570.

Carslaw, D.C., Williams, M.L., Barratt, B., 2012. A short-term intervention study – impact of airport closure due to the eruption of Eyjafjallajökull on near-field air quality. Atmos. Environ. 54, 328–336.

Chen, L., Guo, B., Huang, J.S., He, J., Wang, H.F., Zhang, S.Y., Chen, S.X., 2018. Assessing air-quality in Beijing-Tianjin-Hebei region: the method and mixed tales of $PM_{2.5}$ and O_3. Atmos. Environ. 193, 290–301.

Chen, Z.Y., Chen, D.L., Wen, W., Zhuang, Y., Kwan, M.P., Chen, B., Zhao, B., Yang, L., Gao, B.B., Li, R.Y., Xu, B., 2019. Evaluating the "2+26" regional strategy for air quality improvement during two air pollution alerts in Beijing: variations in $PM_{2.5}$ concentrations, source apportionment, and the relative contribution of local emission and regional transport. Atmos. Chem. Phys. 19, 6879–6891.

Cheng, J., Su, J.P., Cui, T., Li, X., Dong, X., Sun, F., Yang, Y.Y., Tong, D., Zheng, Y.X., Li, Y.S., Li, J.X., Zhang, Q., He, K.B., 2019. Dominant role of emission reduction in $PM_{2.5}$ air quality improvement in Beijing during 2013-2017: a model-based decomposition analysis. Atmos. Chem. Phys. 19, 6125–6146.

Chinese State Council, 2013. Action Plan for the Prevention and Control of Air Pollution. available at: (in Chinese). http://www.gov.cn/zwgk/2013-09/12/content_2486773.htm.

Chinese State Council, 2018. Three-Year Action Plan to Beat Air Pollution. available at: (in Chinese). http://www.gov.cn/zhengce/content/2018-07/03/content_5303158.htm.

Crouse, D.L., Peters, P.A., Donkelaar, A.v., Goldberg, M.S., Villeneuve, P.J., Brion, O., Khan, S., Atari, D.O., Jerrett, M., Pope, C.A., Brauer, M., Brook, J.R., Martin, R.V., Stieb, D., Burnett, R.T., 2012. Risk of nonaccidental and cardiovascular mortality in relation to long-term exposure to low concentrations of fine particulate matter: a canadian national-level cohort study. Environ. Health Perspect. 120, 708–714.

Daskalakis, N., Tsigaridis, K., Myriokefalitakis, S., Fanourgakis, G.S., Kanakidou, M., 2016. Large gain in air quality compared to an alternative anthropogenic emissions scenario. Atmos. Chem. Phys. 16, 9771–9784.

De'ath, G., 2007. Boosted trees for ecological modeling and prediction. Ecology 88, 243–251.

Ding, D., Xing, J., Wang, S.X., Liu, K.Y., Hao, J.M., 2019. Estimated Contributions of Emissions Controls, Meteorological Factors, Population Growth, and Changes in Baseline Mortality to Reductions in Ambient $PM_{2.5}$ and $PM_{2.5}$-Related Mortality in China, 2013-2017. Environ. Health Persp. https://doi.org/10.1289/EHP4157

Dominici, F., McDermott, A., Zeger, S.L., Samet, J.M., 2002. On the use of generalized additive models in time-series studies of air pollution and health. Am. J. Epidemiol. 156, 193–203.

Elith, J., Leathwick, J.R., Hastie, T., 2008. A working guide to boosted regression trees. J. Anim. Ecol. 77, 802–813.

Environmental statistics group in Center for Statistical Science, 2019. Air Quality Assessment Report (6): Regional Pollution Assessment in "2+43" Cities from 2013 to 2018. Peking University (in Chinese).

Geng, G.N., Zhang, Q., Martin, R.V., van Donkelaar, A., Huo, H., Che, H.Z., Lin, J.T., He, K.B., 2015. Estimating long-term $PM_{2.5}$ concentrations in China using satellite-based aerosol optical depth and a chemical transport model. Remote Sens. Environ. 166, 262–270.

Grange, S.K., Carslaw, D.C., Lewis, A.C., Boleti, E., Hueglin, C., 2018. Random forest meteorological normalisation models for Swiss PM_{10} trend analysis. Atmos. Chem. Phys. 18, 6223–6239.

Guo, Y.M., Zeng, H.M., Zheng, R.S., Li, S.S., Barnett, A.G., Zhang, S.W., Zou, X.N., Huxley, R., Chen, W.Q., Williams, G., 2016. The association between lung cancer incidence and ambient air pollution in China: a spatiotemporal analysis. Environ. Res. 144, 60–65.

Henneman, L.R.F., Liu, C., Hu, Y.T., Mulholland, J.A., Russell, A.G., 2017. Air quality modeling for accountability research: operational, dynamic, and diagnostic evaluation. Atmos. Environ. 166, 551–565.

Legates, D.R., McCabe, G.J., 2013. A refined index of model performance: a rejoinder. Int. J. Climatol. 33, 1053–1056.

Liang, X., Li, S., Zhang, S.Y., Huang, H., Chen, S.X., 2016. $PM_{2.5}$ data reliability, consistency, and air quality assessment in five Chinese cities. J. Geophys. Res. Atmos. https://doi.org/10.1002/2016JD024877.

Liang, X., Zou, T., Guo, B., Li, S., Zhang, H.Z., Zhang, S.Y., Huang, H., Chen, S.X., 2015. Assessing Beijing's $PM_{2.5}$ pollution: severity, weather impact, APEC and winter heating. Proc. Res. Soc. A. https://doi.org/10.1098/rspa.2015.0257.

Liu, J., Mauzerall, D.L., Chen, Q., Zhang, Q., Song, Y., Peng, W., Klimont, Z., Qiu, X.H., Zhang, S.Q., Hu, M., Lin, W.L., Smith, K.R., Zhu, T., 2016. Air pollutant emissions from Chinese households: a major and underappreciated ambient pollution source. Proc. Natl. Acad. Sci. 113, 7756–7761.

Maji, K.J., Dikshit, A.K., Arora, M., Deshpande, A., 2018. Estimating premature mortality attributable to $PM_{2.5}$ exposure and benefit of air pollution control policies in China for 2020. Sci. Total Environ. 612, 683–693.

MEP, 2017. 2017 air pollution prevention and control plan for the Beijing-Tianjin-Hebei region and its surrounding areas. available at:, (in Chinese). http://dqhj.mee.gov.cn/dtxx/201703/t20170323_408663.shtml.

MEP, 2020. Civilian bulk coal governance is still a key direction that BTH region and its surrounding areas need to adhere to. http://www.mee.gov.cn/ywgz/dqhjbh/dqhjzlgl/202003/t20200310_768238.shtml.

Pascal, M., Falq, G., Wagner, V., Chatignoux, E., Corso, M., Blanchard, M., Host, S., Pascal, L., Larrieu, S., 2014. Short-term impacts of particulate matter (PM_{10}, $PM_{10-2.5}$, $PM_{2.5}$) on mortality in nine French cities. Atmos. Environ. 95, 175–184.

Pope, C.A., Hansen, J.C., Kuprov, R., Sanders, M.D., Anderson, M.N., Eatough, D.J., 2011. Vascular function and short-term exposure to fine particulate air pollution. J. Air. Waste. Manage. 61, 858–863.

Sahu, S.K., Gelfand, A.E., Holland, D.M., 2006. Spatio-temporal modeling of fine particulate matter. J. Agric. Biol. Environ. Stat. https://doi.org/10.1198/108571106X95746.

Suleiman, A., Tight, M.R., Quinn, A.D., 2016. Hybrid neural networks and boosted regression tree models for predicting roadside particulate matter. Environ. Model. Assess. 21, 731–750.

Tang, Q., Lei, Y., Chen, X.J., Xue, W.B., 2017. Air quality improvement scenario for China during the 13th five-year plan period. Asian J. Atmos. Environ. 11, 33–36.

Tian, H.Z., Hao, J.M., Hu, M.Y., Nie, Y.F., 2007. Recent trends of energy consumption and air pollution in China. J. Energy Eng. 133, 4–12.

Vu, T.V., Shi, Z., Cheng, J., Zhang, Q., He, K., Wang, S., Harrison, R.M., 2019. Assessing the impact of clean air action on air quality trends in Beijing using a machine learning technique. Atmos. Chem. Phys. 19, 11303–11314.

Wang, S.X., Xing, J., Zhao, B., Jang, C., Hao, J.M., 2014. Effectiveness of national air pollution control policies on the air quality in metropolitan areas of China. J. Environ. Sci. 26, 13–22.

Willmott, C.J., 1982. Some comments on the evaluation of model performance. Bull. Am. Meteorol. Soc. 63, 1309–1313.

Xiao, Q.Y., Ma, Z.W., Li, S.S., Liu, Y., 2015. The impact of winter heating on air pollution in China. PloS One 10. https://doi.org/10.1371/journal.pone.0117311.

Yu, S.C., Eder, B., Dennis, R., Chu, S.H., Schwartz, S.E., 2006. New unbiased symmetric metrics for evaluation of air quality models. Atmos. Sci. Lett. 7, 26–34.

Zhai, S.X., Jacob, D.J., Wang, X., Shen, L., Li, K., Zhang, Y.Z., Gui, K., Zhao, T.L., Liao, H., 2019. Fine particulate matter ($PM_{2.5}$) trends in China, 2013-2018: separating contributions from anthropogenic emissions and meteorology. Atmos. Chem. Phys. 19, 11031–11041.

Zhang, Q., He, K.B., Huo, H., 2012. Cleaning China's air. Nature 484, 161–162.

Zhang, Q., Zheng, Y.X., Tong, D., Shao, M., Wang, S.X., Zhang, Y.H., Xu, X.D., Wang, J.N., He, H., Liu, W.Q., Ding, Y.H., Lei, Y., Li, J.H., Wang, Z.F., Zhang, X.Y., Wang, Y.S., Cheng, J., Liu, Y., Shi, Q.R., Yan, L., Geng, G.N., Hong, C.P., Li, M., Liu, F., Zheng, B., Cao, J.J., Ding, A.J., Gao, J., Fu, Q.Y., Huo, J.T., Liu, B.X., Liu, Z.R., Yang, F.M., He, K.B., Hao, J.M., 2019a. Drivers of improved $PM_{2.5}$ air quality in China from 2013 to 2017. Proc. Natl. Acad. Sci. 116, 24463–24469.

Zhang, S.Y., Guo, B., Dong, A.L., He, J., Xu, Z.P., Chen, S.X., 2017. Cautionary tales on air-quality improvement in Beijing. Proc. Math. Phys. Eng. Sci. 473 https://doi.org/10.1098/rspa.2017.0457.

Zhang, X.Y., Xu, X.D., Ding, Y.H., Liu, Y.J., Zhang, H.D., Wang, Y.Q., Zhong, J.T., 2019b. The impact of meteorological changes from 2013 to 2017 on $PM_{2.5}$ mass reduction in key regions in China. Sci. China Earth Sci. 62, 1885–1902.